

CrystEngComm

Accepted Manuscript



This is an *Accepted Manuscript*, which has been through the Royal Society of Chemistry peer review process and has been accepted for publication.

Accepted Manuscripts are published online shortly after acceptance, before technical editing, formatting and proof reading. Using this free service, authors can make their results available to the community, in citable form, before we publish the edited article. We will replace this *Accepted Manuscript* with the edited and formatted *Advance Article* as soon as it is available.

You can find more information about *Accepted Manuscripts* in the [Information for Authors](#).

Please note that technical editing may introduce minor changes to the text and/or graphics, which may alter content. The journal's standard [Terms & Conditions](#) and the [Ethical guidelines](#) still apply. In no event shall the Royal Society of Chemistry be held responsible for any errors or omissions in this *Accepted Manuscript* or any consequences arising from the use of any information it contains.

ARTICLE

Molecular tectonics: dimensionality and geometry control of silver coordination networks based on pyrazolyl appended thiacalixarenes

hCite this: DOI:
10.1039/x0xx00000x

Received 00th January 2012,
Accepted 00th January 2012

DOI: 10.1039/x0xx00000x

www.rsc.org/

A.S. Ovsyannikov,^{a,b,c} M. H. Noamane,^{b,d}, R. Abidi,^d S. Ferlay,^{*b} S. E. Solovieva,^{a,c} I. S. Antipin,^{a,c} A. I. Konovalov,^{a,c} N. Kyritsakas,^b M. W. Hosseini^{*b}

Combinations of six new coordinating tectons (**3-8**) tetrakis-pyrazolyl appended calix[4]arenes, blocked in *1,3-A* conformation, based on **1** (tetrathiacalix[4]arene) and **2** (tetrathiatetramercaptocalix[4]arene) derivatives, with AgX salts (X = NO₃⁻, BF₄⁻, XF₆⁻ (X = P, As and Sb)) lead to nine new silver coordination networks. The flexible nature of tectons **3-8** (length of the spacer between the macrocycle and the pyrazolyl coordinating unit), their high number of potential coordinating sites and the loose coordination demand of Ag⁺ cation lead to the formation of a large variety of networks with different dimensionality: from 1D (**5**-AgSbF₆, **5**-AgBF₄, **7**-AgSbF₆ and **8**-AgNO₃) to extended 2D (**6**-AgBF₄ and **8**-AgSbF₆) and to a series of three isostructural porous diamond-like 3D architectures (**6**-AgXF₆ (X = P, As and Sb)).

Introduction

The design of crystals and development of crystal synthesis are challenging issues of current interest. These two aspects have been subjects of crystal engineering,¹ a research area at the frontier between solid state and supramolecular chemistry.² Indeed, as stated by J. Dunitz, crystals, extended periodic assemblies, may be considered as supermolecules³ for which the components are assembled by attractive intermolecular interactions. However, owing to the complexity of molecular crystal generation, except for some specific combinations of molecular components, the prediction of crystal structure remains in general illusory. Molecular tectonics is an alternative solution to crystal synthesis.⁴ However, this approach is more restrictive since its aim is to design and generate molecular networks, periodic molecular architecture, in the crystalline phase.^{5,6} In other terms, molecular tectonics is not concerned with crystal structure prediction but with the control, under self-assembly conditions, of connectivity between informed and programmed molecular building blocks or tectons through iterative molecular recognition processes.^{4,7}

Among many possible intermolecular or ion-molecule interactions that can be employed for the design of molecular networks, coordination bonds have been extensively used to generate a subclass of molecular networks called coordination polymers,⁸ coordination networks⁹ or metal organic frameworks.¹⁰ Since *ca* two and half decades, this class of crystalline materials has been attracting considerable interest and continue to do that.¹¹ Coordination networks are extended periodic architectures combining organic coordinating tectons and metal centres or metal complexes as metallatectons. For the design of coordinating tectons, calix[4]arene (CA)¹² and its sulphur analogue tetrathiacalix[4]arene TCA,¹³ (compound **1**, Figure 1) and tetramercaptocalix[4]arene^{14,15} and tetramercaptotetrathiacalix[4]arene TMTCA (compound **2**, Figure 1)^{16,17} are interesting macrocyclic backbones. Both molecules are not planar but adopt four interconvertible limit conformations (cone, partial cone, *1,2*-alternate and *1,3*-alternate). Whereas the cone conformer may be used for the generation of discrete assemblies,^{18,19,20} all other three conformer (partial cone, *1,2*-alternate and *1,3*-alternate) may be used as coordinating tectons for the formation of extended coordination networks. Periodic infinite 1-, 2- and 3-D silver

coordination networks based on thiacalix[4]arene derivatives in *1,3*-alternate conformation bearing four nitrile groups,²¹ carboxylate units²² or benzonitrile groups²³ have been described. Another type of 1D silver network based on a TCA derivative, bearing ether junctions, has been also reported.²⁴ The formation of Cu(I) coordination networks based on TCA has been described.²⁵ Infinite architectures based on combinations of TCA derivatives bearing carboxylate groups with metal cations and auxiliary ligands have been also described.²⁶

The coordination ability of TMTCA has been studied and few discrete complexes²⁷ as well as examples of Hg(II), Fe(II), Cd(II) or Ag(I) coordination networks based on pyridyl appended TMTCA derivatives in *1,3*-alternate conformation have been reported.^{28,29,30}

As stated above, although *molecular tectonics* focuses on the design and synthesis of molecular networks in the crystalline phase, as for crystal engineering, except for combinations of rigid complementary tectons (restricted conformational space) with well defined recognition events between them, for flexible tectons offering a large conformational space and different possible recognition modes, the prediction of the connectivity and geometry of networks remains impossible. However, one may discover the formation of periodic extended architectures through systematic experimental explorations based on variations of tectons flexibility and binding ability. In particular, for coordination networks, one may design a series of structurally related coordinating tectons and investigate their combinations with metal connectors.

Here, we report on combinations of a series of 6 new neutral tetrapyrzolylyl appended tectons **3-8** based on thiacalixarene TCA (**3-5**) and tetramercaptothiacalixarene TMTCA (**6-8**) backbones in *1,3-A* conformation (Figure 1) with different silver salts.

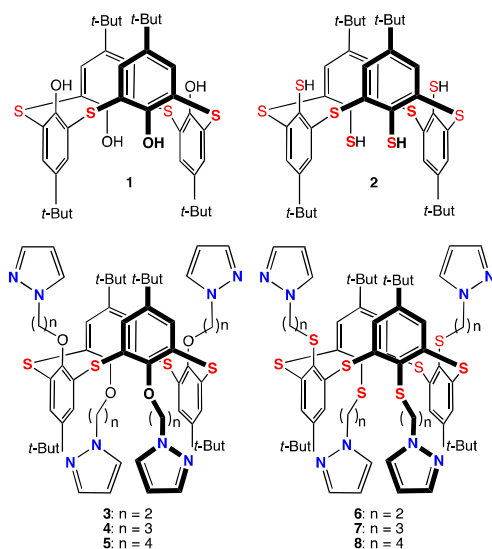


Figure 1: TCA **1** and TMTCA **2** in *1,3-A* conformation as well as pyrazolyl appended tectons **3-8**.

Experimental section

Characterization techniques

¹H-NMR and ¹³C-NMR spectra were recorded at room temperature on a Bruker 300 MHz and 500 MHz spectrometers by the shared NMR Service.

FT-IR spectra were recorded on a Perkin Elmer ATR spectrometer.

Mass spectra (MS (ES+)) were obtained on a Bruker MicroTOF spectrometer by the shared Mass Spectrometry Service.

Melting points were measured in capillary on a Stuart Scientific Melting Point SMP-1 apparatus.

Microanalyses were performed by the shared Elemental Analysis Service.

Synthesis

General: All reagents were purchased from commercial sources and used without further purification. *p*-tert-butylthiacalix[4]arene (TCA) **1**³¹ and *p*-tert-butyltetramercaptothiacalix[4]arene (TMTCA) **2**¹⁶ were prepared following reported procedures.

1-(2-bromoethyl)-1H-pyrazole³²

To a stirred solution of pyrazole (0.5 g, 7.3 mmol) in DMSO (50 mL) KOH (4.12 g, 73 mmol) was added at room temperature. After stirring for 1 h, 1,2-dibromoethane (12.7 mL, 146 mmol) was added and the mixture stirred for 2 hours before water (50 mL) was added. The mixture was extracted with EtOAc (50 mL) and CH₂Cl₂ (50 mL). The combined organic layers were washed with brine (100 mL) and dried over anhydrous MgSO₄, filtered and volatiles were evaporated. The liquid residue thus obtained was purified by flash column chromatography on SiO₂ (cyclohexane/EtOAc 1/1 mixture) affording the pure 1-(2-bromoethyl)-1H-pyrazole (0.77 g) in 60 % yield. ¹H-NMR δ (CDCl₃, 300 MHz): 3.72 (2H, t, Br-CH₂-), 4.50 (2H, t, -CH₂-Pyr), 6.26 (1H, t, Pyr-H), 7.46 (1H, d, Pyr-H), 7.55 (1H, d, Pyr-H).

1-(4-bromobutyl)-1H-pyrazole

To a stirred solution of pyrazole (0.5 g, 7.3 mmol) in DMSO (50 mL) KOH (4.12 g, 73 mmol) was added at room temperature. After stirring for 1 h, 1,4-dibromobutane (31.82 g, 17.6 mL, 146 mmol) was added in one portion and the mixture further stirred for 2 hours. To the reaction mixture water (50 mL) was added and the desired product was extracted with EtOAc (50 mL) and CH₂Cl₂ (50 mL). The combined organic layers were washed with brine (100 mL) and dried over anhydrous MgSO₄, filtered and the evaporated under vacuum. The liquid residue thus obtained was purified by flash column chromatography on Al₂O₃ (cyclohexane/EtOAc 1/1 mixture) affording the pure 1-(4-bromobutyl)-1H-pyrazole (0.97 g) in 65 % yield. ¹H-NMR δ (CDCl₃, 300 MHz): 1.84 (2H, m, Br-CH₂-CH₂-), 2.02 (2H, m, -CH₂-CH₂-Pyr), 3.39 (2H, t, Br-CH₂-), 4.18 (2H, t, -CH₂-Pyr), 6.24 (1H, t, Pyr-H), 7.37 (1H, d, Pyr-H), 7.50 (1H, d, Pyr-H).

25,26,27,28-tetrakis[(3-bromoethyl)]-5,11,17,23-tetra-*tert*-butyl-2,8,14,20-thiacalix[4]arene (3[']) (see figure 2)³³

Under argon, a mixture of TCA **1** (2.0 g, 2.77 mmol) and PPh₃ (7.27 g, 27.73 mmol) in dry THF (20 mL) was stirred at 0 °C for 20 mn. Then, 2-bromoethanol (3.64 g, 2.06 mL, 27.73 mmol) in dry 10 mL of THF was added dropwise. After stirring for 30 mn, a solution of DIAD (Diisopropyl Azodicarboxylate) (5.72 g, 5.57 mL, 27.73 mmol) in dry THF (10 mL) was added dropwise. The reaction mixture was stirred under argon, at room temperature, during 24 hours before it was evaporated to dryness. The residue was treated with MeOH (100 ml) affording the desired compound **3'** in *1,3-A* conformation as a white powder (2.8 g, 89 % yield). mp = > 320 °C. ¹H-NMR (CDCl₃, 500 MHz) δ (ppm) = 1.31 (36H, s, C(CH₃)₃), 2.56 (8H, t, Br-CH₂-), 4.11 (8H, t, -CH₂-O-), 7.36 (8H, s, Ar-*H*). ¹³C-NMR (CDCl₃, 125 MHz) δ (ppm) = 31.6, 34.7, 67.3, 127.4, 128.1, 147.5, 153.4.

25,26,27,28-tetrakis[(3-bromopropyl)]-5,11,17,23-tetra-*tert*-butyl-2,8,14,20-thiacalix[4]arene(4['])

Under argon, a mixture of TCA **1** (1.0 g, 1.38 mmol) and PPh₃ (3.67 g, 13.86 mmol) in dry THF (20 mL) was stirred at 0 °C. Then 3-bromo-1-propanol (1.98 g, 1.29 mL, 13.86 mmol) in dry THF (10 mL) was added dropwise to the mixture. After further stirring for 30 mn, a solution of DIAD (Diisopropyl Azodicarboxylate) (2.85 g, 2.78 mL, 13.86 mmol) in dry THF (10 mL) was added dropwise. The reaction mixture was stirred for 24 hours at room temperature under argon before it was evaporated. The residue was treated with MeOH (100 ml) affording the desired compound **4'** in *1,3-A* conformation as a white powder, (1.67 g, 91 % yield). mp > 320 °C. ¹H-NMR (CDCl₃, 500 MHz) δ (ppm) = 1.32 (36H, s, C(CH₃)₃), 1.55 (8H, m, -CH₂-), 3.07 (8H, t, Br-CH₂-CH₂-), 3.98 (8H, t, -CH₂-O-), 7.37 (8H, s, Ar-*H*). ¹³C-NMR (CDCl₃, 125 MHz) δ (ppm) = 30.5, 31.4, 32.2, 34.5, 67, 127.2, 128.1, 146.5, 156.3.

25,26,27,28-tetrakis[(3-chlorobutyl)]-5,11,17,23-tetra-*tert*-butyl-2,8,14,20-thiacalix[4]arene (5['])

Under argon, a mixture of TCA **1** (1.0 g, 1.38 mmol) and PPh₃ (4.40 g, 16.64 mmol) in dry THF (20 mL) was stirred at 0 °C. Then 4-chloro-1-butanol (2.12 g, 1.95 mL, 16.64 mmol) in dry THF (10 mL) was added dropwise. After stirring for 30 mn, a solution of DIAD (Diisopropyl Azodicarboxylate) (3.39 g, 3.30 mL, 16.64 mmol) in dry THF (10 mL) was added dropwise. The reaction mixture was stirred at room temperature for 24 hours under argon before it was evaporated. The residue was treated with MeOH (100 ml) affording the desired compound **5'** in *1,3-A* conformation as a white powder (1.31 g, 88 % yield). mp > 320 °C. ¹H-NMR (CDCl₃, 300 MHz) δ (ppm) = 1.19 (36H, s, C(CH₃)₃), 1.19 (8H, m, -CH₂-), 1.50 (8H, m, -CH₂-), 3.30 (8H, t, Cl-CH₂-CH₂-), 3.76 (8H, t, CH₂-O-), 7.24 (8H, s, Ar-*H*). ¹³C-NMR (CDCl₃, 125 MHz) δ (ppm) = 30.4, 31.3, 32.2, 34.4, 67.0, 125.2, 128.1, 146.4, 156.3.

25,26,27,28-tetrakis[(3-bromopropyl)thio]-5,11,17,23-tetra-*tert*-butyl-2,8,14,20-tetrathiacalix[4]arene (7['])³⁴

Under argon, a mixture of TMTCA **2** (0.4 g, 0.51 mmol) and Cs₂CO₃ (3.32 g, 10.2 mmol) in dry and degassed acetone (60 mL) was refluxed for 2 hours. Then, 1,3-dibromopropane (1 mL, 10.2 mmol) was added. The reaction mixture was refluxed for 60 hours under argon. After cooling, the reaction mixture was filtrated and the organic solution was evaporated to dryness. The crude residue was recrystallized from a CH₂Cl₂-MeOH 1/10 mixture (50 mL) affording to desired pure product **7'** in *1,3-A* conformation as a white solid (0.52 g, 80 % yield). mp = 310 °C (decomp.) ¹H-NMR (CDCl₃, 300 MHz): 1.32 (36H, s, C(CH₃)₃), 1.89 (8H, m, -CH₂-), 3.06 (8H, t, -CH₂-Br), 3.71 (8H, t, -S-CH₂-), 7.69 (8H, s, Ar-*H*). ¹³C-NMR (125 MHz, CDCl₃): 30.5, 31.4, 32.3, 34.5, 67.1, 127.3, 128.2, 146.5, 156.3.

25,26,27,28-tetrakis[(1-ethyl-1*H*-pyrazole)]-5,11,17,23-tetra-*tert*-butyl-2,8,14,20-thiacalix[4]arene (3)

A mixture of pyrazole (0.36 g, 5.23 mmol) and NaH (0.21 g, 5.23 mmol) was stirred at room temperature in dry DMF (50 mL) for 1 hour. Then **3'** (0.5 g, 0.43 mmol) was added and the solution was heated to 100 °C and stirred for 12 h. The solvent was evaporated to dryness and the residue was dissolved in CHCl₃ (50 mL) and washed with NaHCO₃ (10%, 50 mL) and with H₂O (3 x 50 mL). CHCl₃ was evaporated and compound **3** in *1,3-A* conformation was obtained as a white solid (0.39 g, 69 % yield) by precipitation in ether (100 ml). mp = 262 °C. ¹H-NMR (CDCl₃, 500 MHz) δ (ppm) = 1.13 (36H, s, C(CH₃)₃), 3.89(8H, t, -CH₂-Pyr), 4.34 (8H, t, O-CH₂-), 6.13 (4H, t, Pyr-*H*), 7.11 (4H, d, Pyr-*H*), 7.40 (8H, s, Ar-*H*), 7.42 (4H, d, Pyr-*H*). ¹³C-NMR (CDCl₃, 125 MHz) δ (ppm) = 31.1, 34.3, 50.3, 67.4, 105.5, 128, 128.2, 128.8, 139.1, 147.3, 156.6. MS (ESI) m/z = 1097.45 (M)⁺, (calculated 1097.46). Anal. Calcd. for C₆₀H₇₂N₈O₄S₄: C, 65.66%, H, 6.61%, N, 10.21%; Found: C, 65.73%, H, 6.70%, N, 10.25%.

25,26,27,28-tetrakis[(1-propyl-1*H*-pyrazole)]-5,11,17,23-tetra-*tert*-butyl-2,8,14,20-thiacalix[4]arene (4)

A mixture of pyrazole (0.27 g, 3.98 mmol) and NaH (0.16 g, 3.98 mmol) was stirred at room temperature in dry DMF (50 mL) for 1 hour. Then **4'** (0.4 g, 0.33 mmol) was added and the solution was stirred and heated to 100 °C for 12h. The solvent was evaporated to dryness, the residue dissolved in CHCl₃ (50 mL) and washed with NaHCO₃ (10 %, 50 mL) and with H₂O (3 x 50 mL) and filtrated. CHCl₃ was removed and the mixture was purified by column chromatography on SiO₂ (EtOAc/cyclohexane = 1/4, R_f = 0.9) affording to a desired product **4** in *1,3-A* conformation as a white powder (0.21 g, 55 % yield). mp = 327 °C. ¹H-NMR (CDCl₃, 300 MHz) δ (ppm) = 1.14 (36H, s, C(CH₃)₃), 1.59 (8H, m, -CH₂-), 3.91 (8H, t, -CH₂-Pyr), 3.91 (8H, t, O-CH₂-), 6.17 (4H, t, Pyr-*H*), 7.26 (4H, d, Pyr-*H*), 7.28 (8H, s, Ar-*H*), 7.44 (4H, d, Pyr-*H*). ¹³C-NMR (CDCl₃, 125 MHz) δ (ppm) = 30.0, 31.2, 34.2, 49.3, 66.4, 105.3, 127.7, 128.1, 128.8, 139.0, 146.2, 156.6. MS (ESI) m/z = 1170.56 [M+H₂O]⁺ (calculated 1170.52). Anal. Calcd. for C₆₄H₈₀N₈O₄S₄: C, 66.63 %, H, 6.99 %, N, 9.71 %; Found: C, 66.53 %, H, 7.13 %, N, 9.50 %.

25,26,27,28-tetrakis[(1-butyl-1*H*-pyrazole)]-5,11,17,23-tetra-*tert*-butyl-2,8,14,20-tetrathiacalix[4]arene (5)

A mixture of pyrazole (0.47 g, 6.9 mmol) and NaH (0.16 g, 6.9 mmol) was stirred at room temperature in dry DMF (50 mL) for 1 hour. Then compound **5'** (0.5 g, 0.46 mmol) was added and the solution was stirred and heated to 100 °C for 12h. The solvent was evaporated to dryness and the residue dissolved in CHCl₃ (50 mL) and washed with NaHCO₃ (10%, 50 mL) and with H₂O (3 x 50 mL). CHCl₃ was removed and the compound **5** in *1,3-A* conformation was obtained as a white powder (0.28 g, 51 % yield) after purification by column chromatography on SiO₂ (CH₂Cl₂/CH₃OH = 97/3, R_f = 0.7). mp = 228 °C. ¹H-NMR (CDCl₃, 300 MHz) δ (ppm) = 1.21 (36H, s, C(CH₃)₃), 1.31 (8H, m, -CH₂-), 1.80 (8H, m, -CH₂-), 3.89 (8H, t, -CH₂-Pyr), 4.03 (8H, t, O-CH₂-), 6.22 (4H, t, Pyr-*H*), 7.31 (4H, d, Pyr-*H*), 7.33 (4H, d, Pyr-*H*), 7.48 (4H, d, Pyr-*H*). ¹³C-NMR (CDCl₃, 125 MHz) δ (ppm) = 26.3, 26.9, 31.4, 34.2, 51.6, 69, 105.3, 128.4, 128.8, 129.3, 139.3, 145.5, 157.5. MS (MALDI-TOF) m/z = 1231.60 [M+Na]⁺ (calculated 1231.57). Anal. Calcd. for C₆₈H₈₈N₈O₄S₄·H₂O: C, 66.52%, H, 7.39%, N, 9.13%; Found: C, 66.64%, H, 7.37%, N, 9.02%.

25,26,27,28-tetrakis[(1-ethyl-1*H*-pyrazole)thio]-5,11,17,23-tetra-*tert*-butyl-2,8,14,20-tetrathiacalix[4]arene (6)

A mixture of TMTCA **2** (0.2 g, 0.25 mmol) and Cs₂CO₃ (1.66 g, 5.1 mmol) in dry and degassed acetone (50 ml) was refluxed for 2 hours. Then 1-(2-bromoethyl)-1*H*-pyrazole (0.45 g, 2.5 mmol) was added and the mixture was refluxed for 60 hours under argon. After cooling, the solid residue was filtrated and washed with CH₂Cl₂ (100 ml). CH₂Cl₂ was evaporated and the mixture was purified by column chromatography on Al₂O₃ (CH₂Cl₂, R_f = 0.5) the pure compound **6** as a white solid (0.15 g, yield 50 %). mp = 255 °C (decomp.). ¹H-NMR δ (CDCl₃, 300 MHz) = 1.17 (36H, s, C(CH₃)₃), 3.47 (8H, t, -CH₂-), 4.18 (8H, t, S-CH₂-), 6.26 (4H, t, Pyr-*H*), 7.54 (4H, d, Pyr-*H*), 7.64 (8H, s, Ar-*H*), 7.70 (4H, d, Pyr-*H*). ¹³C-NMR δ (CDCl₃, 125 MHz) = 30.9, 34.5, 35.9; 52.0, 105.1, 130.7, 135.9, 139.6, 139.8, 142.3, 150.3. MS (MALDI-TOF) m/z = 1161.77 (M)⁺ (calculated 1161.37), 1184.39 (M+Na)⁺ (calculated 1184.36). Anal. Calcd. for C₆₀H₇₂N₈S₈: C, 62.03%, H, 6.25%, N, 9.64% ; Found: C, 62.61%, H, 6.32%, N, 9.69%.

25,26,27,28-tetrakis[(1-propyl-1*H*-pyrazole)thio]-5,11,17,23-tetra-*tert*-butyl-2,8,14,20-tetrathiacalix[4]arene (7)

A mixture of pyrazole (0.26 g, 3.8 mmol) and NaH (0.1 g, 4.26 mmol) was stirred at room temperature in dry DMF (50 mL) for 1 hour. Then compound **7'** (0.25 g, 0.2 mmol) was added. The reaction mixture was stirred at the room temperature and under argon during 48 hours. The solvent was evaporated to dryness and the solid residue was washed with CH₂Cl₂ (50 mL) and filtrated. The solvent was removed and the desired compound **7** was obtained as a white powder after treating the crude residue with MeOH (50 ml) (0.15 g, 62% yield). mp = 210 °C (decomp.). ¹H-NMR δ (CDCl₃, 300 MHz): 1.24 (36H, s, C(CH₃)₃), 1.94 (8H, m, -CH₂-), 2.85 (8H, t, -CH₂-), 4.37 (8H, t, S-CH₂-), 6.19 (4H, t, Pyr-*H*), 7.35 (4H, d, Pyr-*H*), 7.50 (4H, d,

Pyr-*H*), 7.69 (8H, s, Ar-*H*). ¹³C-NMR δ (CDCl₃, 125 MHz): 30.2, 31.2, 32.3, 34.7, 50.9, 105.3, 129.7, 133.9, 139.5, 139.7, 142.5, 150.5. MS (MALDI-TOF) m/z = 1239.4 [M+Na]⁺ (calculated 1240.42). Anal. Calcd. for C₆₄H₈₀N₈S₈: 63.12%, H, 6.62%, N, 9.20%; Found: 63.45%, H, 6.85%, N, 9.30%.

25,26,27,28-tetrakis[(1-butyl-1*H*-pyrazole)thio]-5,11,17,23-tetra-*tert*-butyl-2,8,14,20-tetrathiacalix[4]arene (8)

A mixture of TMTCA **2** (0.2 g, 0.25 mmol) and Cs₂CO₃ (1.66 g, 5.1 mmol) in dry and degassed acetone (50 mL) was refluxed for 2 hours. Then 1-(4-bromobutyl)-1*H*-pyrazole (0.52 g, 2.5 mmol) was added and the mixture was refluxed for 60 hours under argon. After cooling, the reaction mixture was filtrated and evaporated. The residue was purified by column chromatography on SiO₂ (cyclohexane/EtOAc = 1/1, R_f = 0.9) and Al₂O₃ (CH₂Cl₂, R_f = 0.5) affording to a desired product **8** as a white powder (0.14 g, 44 % yield). mp = 265 °C (decomp.). ¹H-NMR δ (CDCl₃, 300 MHz) = 1.21 (36H, s, C(CH₃)₃), 1.43 (8H, m, -CH₂-), 2.09 (8H, m, X-CH₂-X), 2.91 (8H, t, X-CH₂-X), 4.19 (8H, t, S-CH₂-), 6.25 (4H, t, Pyr-*H*), 7.39 (4H, d, Pyr-*H*), 7.52 (4H, d, Pyr-*H*), 7.66 (4H, d, Pyr-*H*). ¹³C-NMR δ (CDCl₃, 125 MHz) = 25.6, 28.9, 30.0, 33.5, 34.3, 50.8, 104.4, 128.0, 133.7, 138.2, 139.6, 141.6, 148.6. MS (MALDI-TOF) m/z = 1273.52 [M]⁺ (calculated 1273.49), 1296.53 [M+Na]⁺ (calculated 1296.49). Anal. Calcd. for C₆₈H₈₈N₈S₈: C, 64.11%, H, 6.96%, N, 8.80%; Found: C, 64.13%, H, 6.94%, N, 8.85%

Crystallization conditions

3: a vial containing 0.5 mL of a CHCl₃ solution of **3** (5 mg, 4.55 x 10⁻³ mmol) was placed in a sealed beaker containing CH₃OH. Slow vapour diffusion at room temperature of CH₃OH produced colourless crystals suitable for X-ray diffraction after several days.

6: 1 mL of a CH₂Cl₂ solution of **6** (5 mg, 4.31 x 10⁻³ mmol) was mixed with 1 ml of CH₃OH. Slow evaporation at room temperature produced colourless crystals suitable for X-ray diffraction after several days.

5-AgSbF₆: In a crystallization tube (20 x 4 mm), a solution of compound **5** (5 mg, 4.13 x 10⁻³ mmol) in CHCl₃ (1 mL) was layered with a CHCl₃/CH₃OH (1/1) mixture (0.1 mL). A solution of AgSbF₆ (4.3 mg, 12.39 x 10⁻³ mmol) in CH₃OH (1 mL) was carefully added. At room temperature, slow diffusion in the dark produced colourless crystals suitable for X-ray diffraction after several days (4.1 mg, 71 % yield). Anal. Calcd. for [C₆₈H₈₈N₈O₄S₄·AgSbF₆·(CHCl₃)₅]: C, 40.78%, H, 4.36%, N, 5.21%. Found: C, 40.05 %, H, 3.98 %, N, 5.75 %.

5-AgBF₄: In a crystallization tube (20 x 4 mm), a solution of compound **5** (5 mg, 4.13 x 10⁻³ mmol) in CH₂Cl₂ (1 mL) was layered with CH₂Cl₂/CH₃OH (1/1) mixture (0.1 mL). A solution of AgBF₄ (2.4 mg, 12.39 x 10⁻³ mmol) in CH₃OH (1 mL) was carefully added. At room temperature, slow diffusion

in the dark produced colourless crystals suitable for X-ray diffraction after several days (3.9 mg, 67 % yield). Anal. Calcd. for $[\text{C}_{68}\text{H}_{88}\text{N}_8\text{O}_4\text{S}_4\text{AgBF}_4\cdot(\text{H}_2\text{O})_3]$: C, 56.00%, H, 6.50%, N, 7.68%; Found: C, 56.54%, H, 6.72%, N, 7.62%.

6-AgBF₄:

In a crystallization tube (diameter 4 mm, height 15 cm), a solution of **6** (3 mg, 2.6×10^{-3} mmol) in CHCl_3 (1 mL) was layered with a $\text{CHCl}_3/\text{iso-PrOH}$ (1/1) mixture (0.1 mL). A solution of AgBF_4 (1 mg, 5.2×10^{-3} mmol) in MeOH (1 mL) was carefully added. Slow diffusion at room temperature and in the dark produced after 2 weeks colourless crystals (2.2 mg, 58 % yield) suitable for X-ray diffraction. Anal. Calcd. for $[(\text{C}_{30}\text{H}_{36}\text{N}_4\text{S}_4\text{AgBF}_4)_2\cdot(\text{H}_2\text{O})_2]$: C, 45.93 %, H, 4.75 %, N, 7.14 %; Found: C, 46.15 %; H, 4.8 %; N, 7.25 %.

6-AgPF₆:

In a crystallization tube (diameter 4 mm, height 15 cm), a solution of **6** (3 mg, 2.6×10^{-3} mmol) in CH_2Cl_2 (1 mL) was layered with a $\text{CH}_2\text{Cl}_2/\text{EtOH}$ (1/1) mixture (0.1 mL). A solution of AgPF_6 (1.3 mg, 5.2×10^{-3} mmol) in EtOH (1 mL) was carefully added. Slow diffusion at room temperature and in the dark produced after 2 weeks colourless crystals (2.2 mg, 51 % yield) suitable for X-ray diffraction. Anal. Calcd. for $[\text{C}_{30}\text{H}_{36}\text{N}_4\text{S}_4\text{AgPF}_6\cdot(\text{H}_2\text{O})_3]$: C, 40.59 %, H, 4.77 %, N, 6.31 %; Found: C, 40.81 %; H, 4.82 %; N, 6.34 %.

6-AgSbF₆:

In a crystallization tube (diameter 4 mm, height 15 cm), a solution of **6** (3 mg, 2.6×10^{-3} mmol) in CH_2Cl_2 (1 mL) was layered with a $\text{CH}_2\text{Cl}_2/\text{EtOH}$ (1/1) mixture (0.1 mL). A solution of AgSbF_6 (1.8 mg, 5.2×10^{-3} mmol) in EtOH (1 mL) was carefully added. Slow diffusion at room temperature and in the dark produced after 2 weeks colourless crystals (2.8 mg, 59 % yield) suitable for X-ray diffraction. Anal. Calcd. for $[\text{C}_{30}\text{H}_{36}\text{N}_4\text{S}_4\text{AgSbF}_6\cdot(\text{H}_2\text{O})_3]$: C, 36.82 %, H, 4.33 %, N, 5.73 %; Found: C, 36.98 %, H, 4.45 %, N, 5.76 %.

6-AgAsF₆:

In a crystallization tube (diameter 4 mm, height 15 cm), a solution of **6** (3 mg, 2.6×10^{-3} mmol) in CH_2Cl_2 (1 mL) was layered with a $\text{CH}_2\text{Cl}_2/\text{EtOH}$ (1/1) mixture (0.1 mL). A solution of AgAsF_6 (1.5 mg, 5.2×10^{-3} mmol) in EtOH (1 mL) was carefully added. Slow diffusion at room temperature and in the dark produced after 2 weeks colourless crystals (2.7 mg, 60 % yield) suitable for X-ray diffraction. Anal. Calcd. for $[\text{C}_{30}\text{H}_{36}\text{N}_4\text{S}_4\text{AgAsF}_6\cdot(\text{H}_2\text{O})_3]$: C, 38.67 %, H, 4.54 %, N, 6.01 %; Found: C, 38.81 %, H, 4.58 %, N, 6.06%.

7-AgSbF₆:

In a crystallization tube (diameter 4 mm, height 15 cm), a solution of **7** (5 mg, 4.1×10^{-3} mmol) in CHCl_3 (1 mL) was layered with a $\text{CHCl}_3/\text{iso-PrOH}$ (1/1) mixture (0.1 mL). A solution of AgSbF_6 (2.8 mg, 8.2×10^{-3} mmol) in MeOH (1 mL) was carefully added. Slow diffusion at room temperature and in the dark produced after 2 weeks colourless crystals (2.5 mg,

53 % yield) suitable for X-ray diffraction. Anal. Calcd. for $[\text{Ag}_2(\text{C}_{64}\text{H}_{80}\text{N}_8\text{S}_8)(\text{SbF}_6)_2\cdot(\text{CHCl}_3)_2]$: C, 36.98 %, H, 3.86 %, N, 5.23 %; Found: C, 37.10 %, H, 3.90 %, N, 5.21 %.

8-AgSbF₆:

In a crystallization tube (20 x 4 mm), a solution of **8** (3 mg, 2.3×10^{-3} mmol) in CHCl_3 (1 mL) was layered with $\text{CHCl}_3/\text{iso-PrOH}$ (1/1) mixture (0.1 mL). A solution of AgSbF_6 (1.6 mg, 4.6×10^{-3} mmol) in MeOH (1 mL) was carefully added. At room temperature, slow diffusion in the dark produced colourless crystals suitable for X-ray diffraction after 1 month (2.0 mg, 43 % yield). Anal. Calcd. for $[\text{Ag}_4(\text{C}_{68}\text{H}_{88}\text{N}_8\text{S}_8)2(\text{SbF}_6)_4\cdot(\text{CHCl}_3)_7\cdot(\text{H}_2\text{O})_2]$: C, 35.83%, H, 3.93%, N, 4.67% Found: C, 36.11 %, H, 4.01 %, N, 4.75 %.

8-AgNO₃:

In a crystallization tube (20 x 4 mm), a solution of **8** (3 mg, 2.3×10^{-3} mmol) in CHCl_3 (1 mL) was layered with $\text{CHCl}_3/\text{iso-PrOH}$ (1/1) mixture (0.1 mL). A solution of AgNO_3 (0.8 mg, 4.6×10^{-3} mmol) in MeOH (1 mL) was carefully added. At room temperature, slow diffusion in the dark produced colourless crystals suitable for X-ray diffraction after 1 month (1.9 mg 50 % yield). Anal. Calcd. for $[\text{C}_{34}\text{H}_{44}\text{N}_4\text{S}_4\text{AgNO}_3\cdot\text{H}_2\text{O}]$: C, 49.51%, H, 5.62%, N, 8.49%; Found: C, 50.12 %, H, 5.70%, N, 8.54%.

Structural studies

Single-Crystal Studies

Data were collected at 173(2) K on a Bruker SMART CCD diffractometer equipped with an Oxford Cryosystem liquid N_2 device, using graphite-monochromated Mo-K α ($\lambda = 0.71073 \text{ \AA}$) radiation. For all structures, diffraction data were corrected for absorption. Structures were solved using SHELXS-97 and refined by full matrix least-squares on F^2 using SHELXL-97. The hydrogen atoms were introduced at calculated positions and refined using a riding model.³⁵ They can be obtained free of charge from the Cambridge Crystallographic Data Centre via www.ccdc.cam.ac.uk/datarequest/cif. CCDC: 1438358-1438368

Powder diffraction studies (PXRD)

Diagrams were collected on a Bruker D8 diffractometer using monochromatic Cu-K α radiation with a scanning range between 4 and 40° using a scan step size of 8°/min. As already demonstrated and currently admitted, for all compounds, discrepancies in intensity between the observed and simulated patterns are due to preferential orientations of the microcrystalline powders.

Results and discussion

Design and preparation of tectons

Analogous tectons **3-5** (Figure 2) are based on the tetrathiacalix[4]arene backbone (TCA) in *1,3-A* conformation. The latter is functionalized with four pyrazolyl moieties

through ether junctions using ethyl (3), propyl (4) and butyl (5) spacers. Tectons 6-8 (figure 2), based on the tetrascaptotetrathiacalix[4]arene backbone (TMTCA) in 1,3-*A* conformation, are sulphur analogues of tectons 3-5 for which the O atoms are replaced by S atoms. Although calix[4]arene derivatives bearing pyrazolyl groups at the upper rim have been reported,³⁶ to the best of our knowledge, no TCA or TMTCA pyrazolyl appended tectons have been described so far in the literature. However, pyrazolyl appended [1,1,1]metacyclophane derivatives in 1,3-*A* conformation and their combinations with metal cation have been previously documented.³⁷ The rationale behind the use of $(-\text{CH}_2)_n$, ($n = 2 - 4$) spacer to connect the calix backbone 1 or 2 to the coordinating pyrazolyl moiety was to investigate the role played by the flexibility of the spacer on the dimensionality and geometry of extended periodic architectures when combined with metal cations such as Ag^+ . The reason for the substitution of the O atoms in 1 (tectons 3 - 5) by S atoms in 2, (tectons 6 - 8) was to study their coordination propensity towards silver cation in the formation of the extended networks. As connecting metallic node, Ag^+ , a d^{10} cation, was used owing to its loose coordination requirements and the reversibility of Ag^+ -N bond formation. Since tectons 3-8 are neutral entities, their combinations with Ag^+ cation leading to the formation of cationic extended networks require the presence of anions for charge neutrality reasons. The role played by the counter ion on the formation of silver coordination networks was investigated by using different silver salts (BF_4^- , XF_6^- ($X = \text{P}, \text{As}$ and Sb)). The synthetic strategy used to prepare compounds 3-8 is presented in figure 2 (see experimental section for details). In order to increase the yield of the desired products in 1,3-*A* conformation, two synthetic pathways have been explored (figure 2).

Using TCA 1 as the starting material, compounds 3, 4 and 5, have been prepared in two steps. The Mitsunobu condensation between compound 1 and α -bromoalcohol $\text{Br}-(\text{CH}_2)_n-\text{OH}$ ($n = 2 - 4$) in dry THF in the presence of DIAD (Diisopropyl Azodicarboxylate) and PPh_3 afforded the tetrabromo intermediates 3' ($n = 2$), 4' ($n = 3$) and 5' ($n = 4$) in 88-91 % yield. The condensation of the latter with pyrazole in dry DMF in the presence of NaH as base afforded the desired tectons 3-5 in 69, 55 and 51 % yield respectively.

Tectons 6 ($n = 2$) and 8 ($n = 4$), have been obtained upon directed condensation of TMTCA 2 with bromalkylpyrazole in dry acetone in the presence of Cs_2CO_3 as base in 50 and 44% yield respectively. Compound 7 was prepared in 62 % yield by condensing the TMTCA derivative 7¹³⁴ with pyrazole in dry DMF in the presence of NaH.

In all cases, only the 1,3-*A* conformation was isolated from the reaction mixtures.

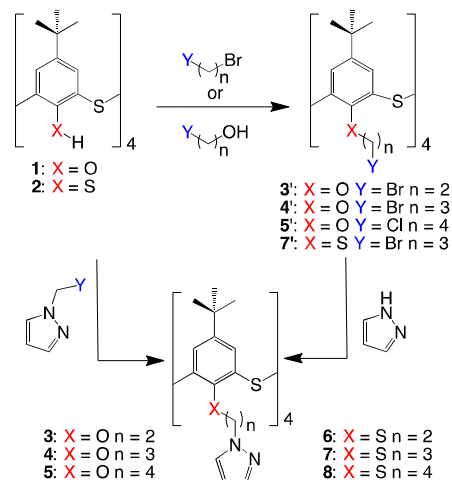


Figure 2: Two different synthetic pathways followed for the preparation of TCA and TMTCA pyrazolyl appended tectons 3 - 8 (for experimental details see experimental section).

In addition to solution characterization of all tectons 3-8, compounds 3 and 6 have been also studied by X-ray diffraction on single crystals (see crystallographic table 1). Crystals of 3 and 6 were obtained upon slow diffusion or slow evaporation techniques (see experimental part). As expected, both compounds are in the 1,3-*A* conformation in the solid state (Figure 3).

Whereas crystals of 3 contain H_2O molecules, 6 crystallises in the absence of solvent molecules. For both cases, the metrics of the macrocyclic part is close to those observed for the parent compound 1¹³ and 2¹⁶ (see table 2). For 3, one out of the four pyrazolyl groups is found to be disordered.

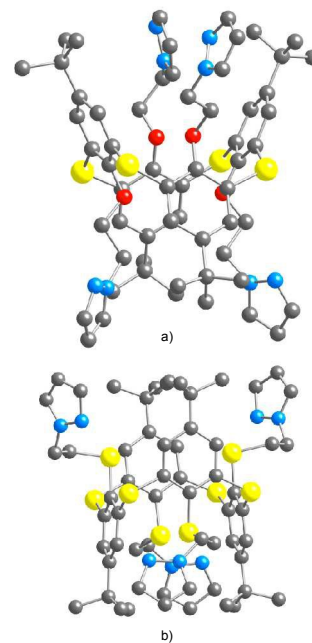


Figure 3: Solid state structures of tectons 3 and 6 in a 1,3-alternate conformation. H atoms and solvent molecules and disordered pyrazolyl groups are not presented for clarity. For bond distances and angles see the text.

Table 2: Distances and angles for compounds **3** and **6** obtained by X-ray diffraction on single crystals.

	3	6
S-C(Ar)	1.763(6)-1.778(6)	1.781(2), 1.784(2) and 1.785(2)
O(S)-Ar	1.363(7)-1.383(7)	1.777(2) and 1.781(2)
N-N (pyrazol)	1.336(11) -1.354(18)	1.348(3) and 1.357(3)

For both compounds, the coordinating pyrazolyl groups are oriented almost perpendicular to the main plane formed by the four S atoms connecting the aromatic rings.

Structural description of the networks

For all four combinations of tectons **3-8** and AgX (X = BF₄⁻, PF₆⁻, SbF₆⁻, NO₃⁻) salts, suitable crystals for X-ray diffraction studies on single crystal were obtained at room temperature using slow evaporation or slow diffusion methods (see Experimental part and crystallographic table 3). For air stable crystals, the purity of the crystalline phase was established by PXRD on microcrystalline powder.

The structural discussion given below is based on increasing dimensionality (1-3D) of silver coordination networks. In all cases, since bond distances and angles observed for the macrocyclic portion of tectons were found to be close to those of the parent compounds **1-3** and **6**, their metrics will not be discussed.

1D networks

For the combinations of the tecton **5** with both AgSbF₆ and AgBF₄ silver salts, two cationic infinite 1-D non-tubular architectures were obtained (Figure 4). The same connectivity observed for both crystalline materials **5-AgSbF₆** and **5-AgBF₄** has been previously observed for combinations of tetrahedral silver cation with other tetra-substituted calix[4]arene^{21,29b} and cyclophane derivatives.³⁸ In both cases, the crystal (space group P2(1)/c for **5-AgSbF₆** and Cc for **5-AgBF₄**) is composed of the neutral tecton **5**, Ag⁺ cation, BF₄⁻ or SbF₆⁻ anion and solvent molecules (CHCl₃ for **5-AgSbF₆** and H₂O for **5-AgBF₄**). No specific interactions between the Ag⁺ cation and anions or solvents were spotted. For both compounds, a 1/1 ligand/metal ratio is obtained. The cationic part of the network is generated by mutual bridging between the tetradentate tecton **5** and silver cation, adopting a tetrahedral coordination geometry, through pyrazolyl-silver interactions (figure 4). The other heteroatoms of **5** (O and S) are not involved in the bonding of the metal cation. The coordination sphere around Ag⁺ cation is composed of four N atoms belonging to two consecutive tectons **5** (Ag-N distances in the 2.272(3) - 2.451(3) Å range for **5-AgSbF₆** and 2.241(8) - 2.465(13) Å for **5-AgBF₄**). The coordination geometry around the cation is a distorted tetrahedron (N-Ag-N angle varying between 87.10(10) and 126.46(12)° for **5-AgSbF₆** and 92.5(4) and 151.7(4)° for **5-AgBF₄**). The distance between

consecutive Ag⁺ cations within the 1D network is *ca.* 16.9 Å for **5-AgSbF₆** and 17.3 Å for **5-AgBF₄**.

The 1-D networks are packed in a parallel fashion along *b* and *c* axis for **5-AgSbF₆** and along *a* and *c* axis for **5-AgBF₄**. No specific interactions between Ag⁺ cation, the organic tecton **5** and solvent molecules (H₂O or CHCl₃) are observed.

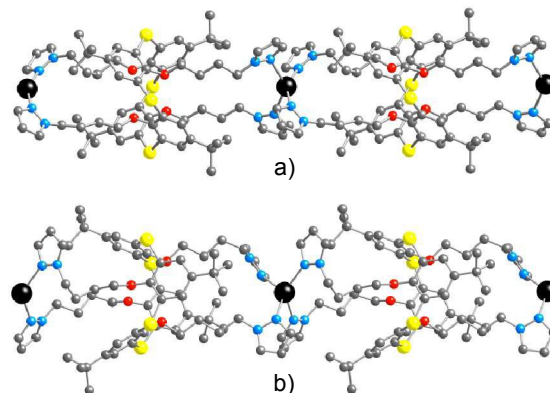


Figure 4: Portions of the solid state structures of 1D silver coordination networks **5-AgBF₄** (a) and **5-AgSbF₆** (b) showing the mutual bridging between the coordinating tecton **5** and silver cation leading to the formation of similar cationic 1-D coordination networks. Silver cations are presented with black spheres. H atoms, anions and solvent molecules are not presented for sake of clarity. For bond distances and angles see text.

Owing to the decomposition of the crystals of **5-AgSbF₆** and **5-AgBF₄** in air, probably due to solvents loss, no XRPD diagrams could be recorded.

Combinations of tecton **7** with AgSbF₆ or **8** with AgNO₃ led to the formation of infinite cationic 1-D architectures with different type of connectivity (Figure 5) when compared to **5-AgSbF₆** and **5-AgBF₄** discussed above. Both networks **7-AgSbF₆** and **8-AgNO₃** display similar type of connectivity around the metal centre. In both cases, crystals (space group *P-1* for **7-AgSbF₆** and *C2/c* for **8-AgNO₃**) are composed of the neutral tecton **7** or **8**, Ag⁺ cations with a 1/2 ligand/metal ratio, SbF₆⁻ or NO₃⁻ anion and solvent molecules (CHCl₃ for **7-AgSbF₆** and H₂O for **8-AgNO₃**). In both cases, the cationic part of the network is generated by mutual interconnection of the tetradentate organic tectons and metal cations adopting a tetrahedral coordination geometry through pyrazol-silver interactions. In marked contrast with **5-AgSbF₆** and **5-AgBF₄** networks, here, in addition to Ag⁺-N interactions, Ag⁺-S bonds are formed (Figure 5a). In the case of **8-AgNO₃**, all three types of Ag⁺-N, Ag⁺-S and Ag⁺-O bonds are observed (Figure 5b).

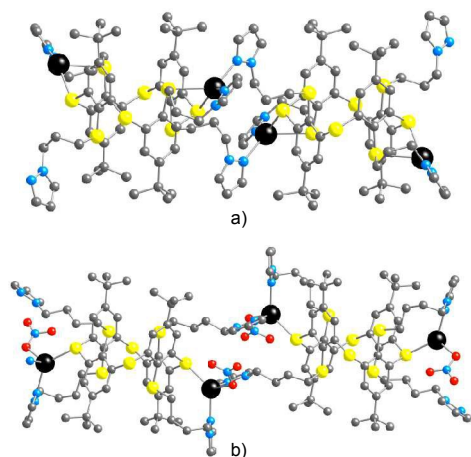


Figure 5: Portions of the solid state structures of of 1D silver coordination networks **7-AgSbF₆** (a) and **8-AgNO₃** (b) showing the mutual bridging between tectons **7** or **8** and silver cation leading to the formation of cationic 1-D coordination networks. Silver cations are presented with black spheres. H atoms, anions and solvent molecules are not presented for sake of clarity. For bond distances and angles see text.

For **7-AgSbF₆**, two crystallographically independent silver cations adopting a tetrahedral coordination geometry and displaying the same coordination sphere composed of two N atoms belonging to two consecutive tectons **7** (Ag-N distances in the 2.210(5) - 2.312(4) Å range) and two sulphur atoms belonging to the thioether groups as well as to the sulphur bridging atom of the thiacalixarene moiety (Ag-S in the 2.5346(13) - 2.9119(14) Å range) are present. The coordination geometry around the cation is again a distorted tetrahedron (N_{Ag}N angles of 101.21(18) and 103.26(18)°, S_{Ag}S angles of 73.07(4) and 74.11(4)°, and N_{Ag}S angles varying between 94.26(13) and 140.88(15)°). For **8-AgNO₃**, only a single type of silver cation is present. The latter is surrounded by two N atoms belonging to two consecutive tectons **8** (Ag-N distances of 2.239(3) - 2.373(3) Å), a sulphur atom of the bridging type with Ag-S distance of 2.5451(8) Å and finally, an oxygen atom belonging to a nitrate anion with Ag-O distance of 2.395(5) Å. Again, the coordination geometry around the cation is a distorted tetrahedron (N_{Ag}N and S_{Ag}O angles of 99.64(12) and 119.31(17)° respectively, N_{Ag}S angles of 94.12(8) and 132.81(9)°, and N_{Ag}O angles of 98.35(17) and 108.99(16)°). The shortest distance between consecutive Ag⁺ cations within the 1-D network is *ca.* 8.64 Å for **7-AgSbF₆** and 7.38 Å for **8-AgNO₃**.

For **7-AgSbF₆**, the 1D arrays are packed in parallel fashion along the [110] and [011] planes with SbF₆⁻ anions and CHCl₃ solvent molecules lying between them. For **8-AgNO₃**, the 1D arrays are packed along the *a* and *b* axes, with water molecules lying between the chains.

The XRPD analysis of **7-AgSbF₆** revealed a good match between simulated and observed patterns indicating the presence of a single microcrystalline phase (Figure 6). Unfortunately, **8-AgNO₃**, probably due to loss of solvent molecules, was found to be unstable in air and thus the purity of the phase could not be established by XRPD.

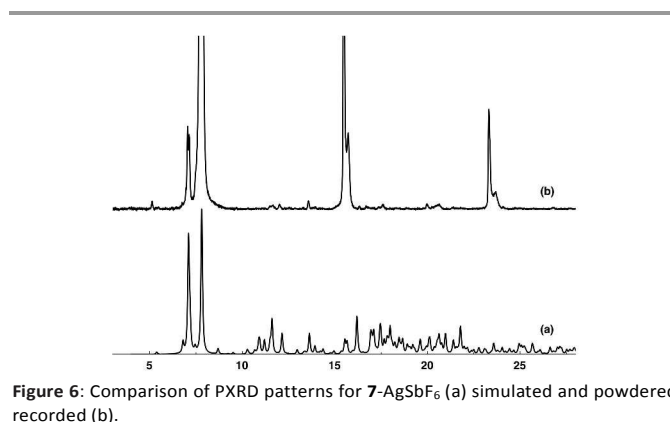


Figure 6: Comparison of PXRD patterns for **7-AgSbF₆** (a) simulated and powdered recorded (b).

2D networks

Two 2D coordination networks **6-AgBF₄** and **8-AgSbF₆** were obtained by combinations of tectons **6** and **8** with silver cation. In both cases, a 1/2 ligand/metal ratio is observed. Crystals are composed of cationic 2D networks, BF₄⁻ and SbF₆⁻ anions in the case of tecton **6** and **8** respectively and solvent molecules (H₂O for **6-AgBF₄** and CHCl₃ for **8-AgSbF₆**).

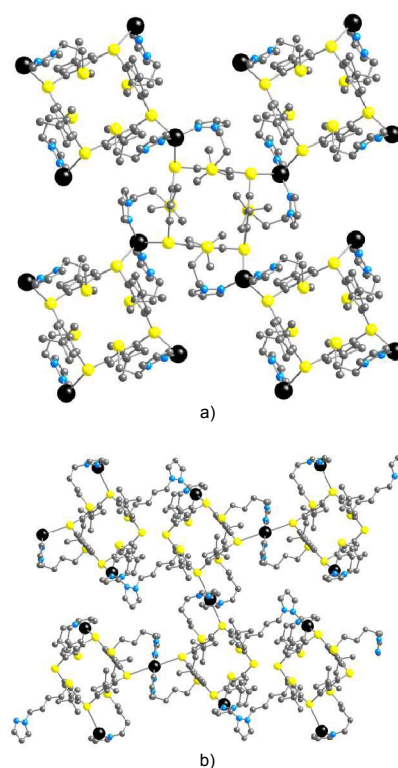


Figure 7: Portions of the solid state structures of **6-AgBF₄** (a) and **8-AgSbF₆** (b) showing the mutual bridging between tectons **6** (a) and **8** (b) with silver cation leading to the formation of cationic 2-D coordination networks. Silver cations are presented with black spheres. H atoms, anions and solvent molecules are not presented for sake of clarity. For bond distances and angles see text.

Whereas **6**-AgBF₄ crystallises in the tetragonal space group *I41/a*, **8**-AgSbF₆ crystallises in the triclinic *P-1* space group. The cationic part of networks is generated by the interconnection of organic tectons **6** or **8** by silver cations (adopting either a triangular or a tetrahedral coordination geometry), through coordination bonds formed between the nitrogen donor atom of pyrazolyl moieties and sulphur atoms belonging to the macrocyclic backbone. In both cases, all four pyrazolyl groups take part in the binding of the cation and thus in the formation of the 2D networks (Figures 7). No specific interactions between silver atoms, anions or the organic tectons **6** or **8** with the solvent molecules were spotted in the crystal.

For the highly symmetrical **6**-AgBF₄ 2D network, the coordination sphere of silver cation is composed of two pyrazolyl nitrogen atoms belonging to two consecutive tectons **6** and two bridging sulphur atoms belonging to two adjacent macrocyclic moieties with Ag-N distances of 2.184(4) and 2.225(5) Å and Ag-S distances of 2.7758(13) and 2.8908(13) Å. (Figure 7a). The coordination geometry around the metal cation is a distorted tetrahedron (N_{Ag}N angle of 152.28(18)°, S_{Ag}S of 95.46(4)° and N_{Ag}S angles varying between 86.31(13) and 115.68(12)°). Along the *c* axis, the 2D networks are packed in parallel and staggered fashion preventing thus the formation of channels. BF₄⁻ anions and water molecules are located between 2D networks.

For the 2D network **8**-AgSbF₆, three crystallographically independent silver cations are present within the network. They all display similar coordination environments composed of two pyrazolyl nitrogen atoms belonging to two different tectons **8** and two bridging sulphur atoms belonging to two adjacent macrocyclic moieties with Ag-N distances varying between 2.092(8) and 2.327(5) Å and Ag-S distances of 2.4503(13) and 3.257(8) Å. Among the three crystallographically independent silver cations, one adopts a deformed tetrahedral coordination geometry (N_{Ag}N angle of 94.48(19)°, S_{Ag}S of 70.44(14)° and N_{Ag}S angle ranging between 148.29(13) and 115.68(12)°). Both other two cations adopt a deformed square geometry (N_{Ag}N and S_{Ag}S angles of 180° and N_{Ag}S angle of 75.29(11)°, 79.64(12)°, 100.35(12) and 104.71(13)°). The 2D networks are packed along the *a* axis, and between the planes are located solvent molecules (CHCl₃ and H₂O) as well as the SbF₆⁻ counter anions.

Probably because of loss of solvent molecules, **6**-AgBF₄ and **8**-AgSbF₆ crystals are unfortunately not stable in air and the purity of solid batches could not be investigated by XRPD.

3D networks

Interestingly combinations of the tecton **6** with three silver salts AgXF₆ (X = P, As and Sb) lead to the formation of three isostructural 3D silver coordination networks **6**-AgXF₆ (X = P, As or Sb). All three extended architectures crystallise in the tetragonal *I41/a* space group with a 1/2 metal/ligand ratio. The three 3D networks differ only by the nature of X in XF₆⁻ anion. Since all three crystals are isostructural, only **6**-AgPF₆ is

described in detail below. However, metrics for the other two crystals **6**-AgAsF₆ and **6**-AgSbF₆ are reported in table 4. The overall structure of **6**-AgPF₆ is of pseudo-diamond type for which tecton **6** behaves as a tetrahedral connector (Figure 8a). The silver cation, adopting a deformed tetrahedral coordination geometry, acts as a two-connecting node each bridging two neighbour tectons **6** (Figures 8).

The surrounding around the silver cation is composed of two nitrogen atoms belonging to pyrazolyl units of different tectons **6** with Ag-N distance of 2.149(12) Å (table 4) and two bridging sulphur atoms belonging to two different tectons **6** with Ag-S distance of 3.040(3) Å. The surrounding of the silver atom is a deformed tetrahedron with N_{Ag}N and S_{Ag}S angles of 170.1(8) and 129.2(7)° respectively and N_{Ag}S angles of 87.1(5) and 97.2(6)°. The 3D pseudo diamond type architecture display channels (13 x 7 Å). The crystal contains two types of water molecules. Whereas as the first type are located between the macrocyclic units along the channel axis, the second type, forming H-bonded dimers (O-O distance of 3.042(7) Å) are within channels (Fig. 8b).

No interactions between the cationic network and the XF₆⁻ (X = P, As and Sb) anions, occupying voids, could be spotted.

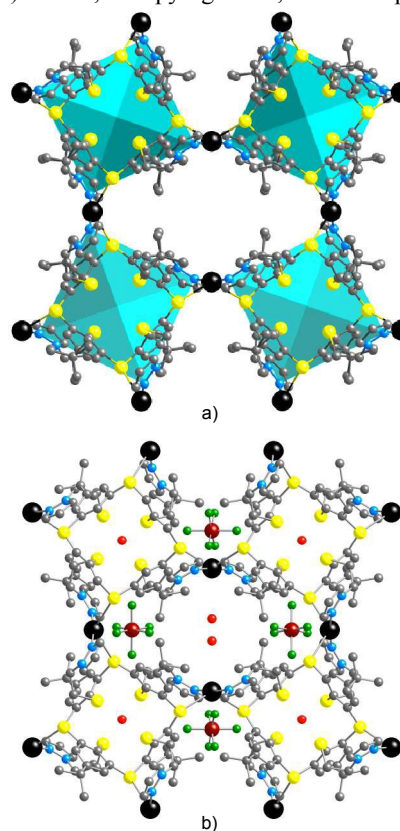


Figure 8: Portions of the solid state structures of **6**-AgPF₆ showing the mutual bridging between silver cations (black spheres) and tectons **6** leading to the formation of a cationic 3-D diamond-like coordination network (a, polyhedral representation) and localizations of water molecules and anions (b). H atoms, anions and solvent molecules are not presented for sake of clarity. For bond distances and angles see text.

Table 4: Selected bond distances and angles for compounds **6**-AgXF₆ (X = P, As and Sb) extracted from the structural study by X ray diffraction on single crystals.

	6 -AgPF ₆	6 -AgAsF ₆	6 -AgSbF ₆
Ag-N (Å)	2.154(5)	2.146(6)	2.163(12)
Ag-S (Å)	3.066(3)	3.067(4)	3.015(4)
NAgN (°)	173.3(3)	173.9(3)	165.3(6)
NAgS (°)	87.5(5)	87.5(5)	85.7(7)
	95.3(6)	95.3(6)	99.4(6)
SAgS (°)	127.4(7)	127.4(7)	139.7(5)
O-O (Å)	3.042(7)	2.876(7)	3.143(7)

The XRPD analysis of microcrystalline samples of **6**-AgAsF₆ and **6**-AgSbF₆ revealed a good match between simulated and observed diagrams implying the presence of single crystalline phases (Figure 9). The XRPD diagram of **6**-AgPF₆ could not be recorded since the compound is not stable in air.

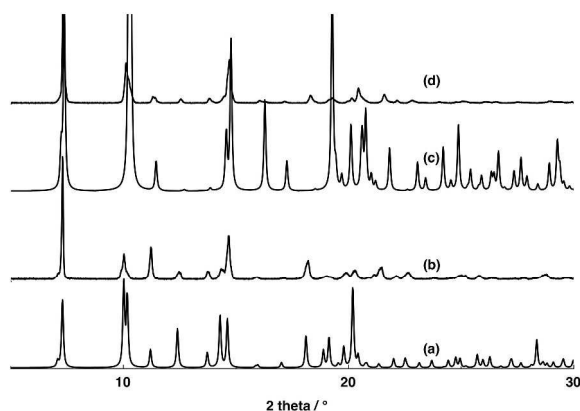


Figure 9: Comparison of XRPD patterns for (a) simulated for **6**-AgSbF₆ (b) recorded for **6**-AgSbF₆ (c) simulated for **6**-AgAsF₆ and (d) recorded for **6**-AgAsF₆.

Discussion

Owing to the flexible nature of organic TCA and TMTCA, in *1,3-A* conformation, based tectons **3-8** and the presence, within their frameworks, of large number of potentially coordinating hetero atoms (N, O and S for **3-5** and N and S for **6-8**), the prediction of connectivity and geometry of coordination networks generated in the presence of silver cation as connecting metal is impossible. However, the nature of the extended architectures in the crystalline phase may be experimentally determined. The present contribution describes systematic investigations on combinations of 6 new tectons **3-8** and different silver salts (NO₃⁻, BF₄⁻, XF₆⁻ (X = P, As and Sb)). Under crystallization conditions used, no crystalline material could be obtained for combinations of tectons **3** and **4** with Ag⁺ cation. For the other tectons **5-8**, 9 extended architectures of different connectivity and geometry have been obtained and characterized in the solid-state. In all cases, all four appended

pyrazolyl coordinating groups participate in the binding of silver cation through Ag-N bonds.

In the case of tecton **5**, independent of the nature of the counter ion (BF₄⁻ or SbF₆⁻), two 1D networks (**5**-AgSbF₆ and **5**-AgBF₄) with similar connectivity pattern (1/1 metal/teuton ratio) have been obtained (Figure 10a). Bridging S atoms do not participate in the binding of silver cations and no specific interactions between anions and the framework were spotted.

The formation of 1D architectures has been also observed upon combining tectons **7** or **8** with silver cation (**7**-AgSbF₆ and **8**-AgNO₃). However, for these two networks a 2/1 metal/teuton ratio is observed (Figure 10b). In contrast with the above mentioned 1D networks obtained with tecton **5**, for both tectons **7** and **8**, S atoms bridging the thiophenol moieties take part in the binding of Ag⁺ cation. In the case of **8**-AgNO₃, NO₃⁻ anions also bind Ag⁺ cation through Ag-O bonds.

In marked contrast, combinations of both tectons **6** and **8** with Ag⁺ cation lead to the formation of similar 2D architectures (**6**-AgBF₄ and **8**-AgSbF₆). Again, a 2/1 metal/teuton ratio is observed (Figure 10c). Again as in the case of **7**-AgSbF₆ and **8**-AgNO₃ mentioned above, S atoms bridging the thiophenol moieties take part in the binding of Ag⁺ cation.

Finally, in contrast with the 2D network obtained upon combining tecton **6** with AgBF₄, its combinations with AgXF₆ (X = P, As or Sb) lead to the formation of porous isostructural crystals based on 3D networks (**6**-AgXF₆ (X = P, As and Sb)) (Figure 10d). Interestingly, the formation of the pseudo diamond type architecture is independent of the nature of the octahedral anion. The porous crystals contain two types of water molecules with inclusion of H-bonded dimers within the channels.

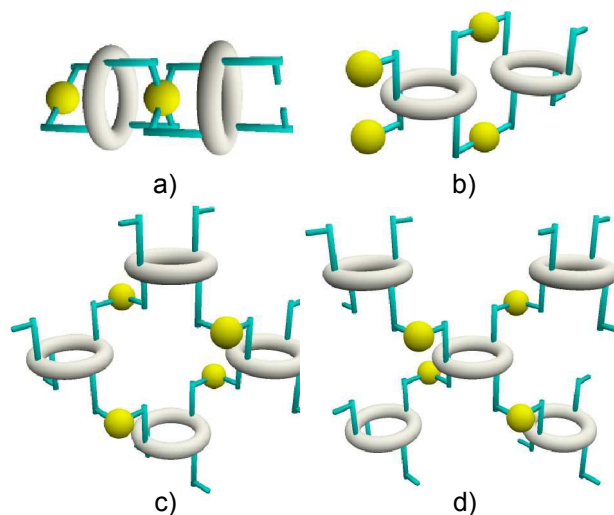


Figure 10: Schematic representation of 1D networks **5**-AgBF₄ and **5**-AgSbF₆ obtained upon combining the organic tecton **5** with silver cation (a), 1D networks **7**-AgSbF₆ and **8**-AgNO₃ obtained upon combining the organic tectons **7** or **8** with silver cation (b), 2D networks **6**-AgBF₄ and **8**-AgSbF₆ obtained upon combining the organic tectons **6** or **8** with silver cation (c), 3D networks **6**-AgXF₆ (X = P, As or Sb) obtained upon combining the organic tectons **6** with silver cation (d). For sake of clarity only Ag⁺-N interactions are represented.

Combinations of calix[4]arene in *1,3-A* conformation based tectons **3-8** with other metal cations are currently under investigation.

Acknowledgments

We thank the Russian Scientific Foundation (grant N° 15-13-30006) for financial support in synthesis and crystal preparation of some of the reported compounds. We thank the Tunisian Ministry of Education for scholarship of M.H.N. Financial supports from the University of Strasbourg, the International Centre for Frontier Research in Chemistry (icFRC), Laboratory of excellence LabEx CSC, Strasbourg, the Institut Universitaire de France, the CNRS are acknowledged.

Notes and references

^a Kazan Federal University, Kremlevskaya str. 18, Kazan 420008, Russian Federation

^b Molecular Tectonics Laboratory, UMR Uds-CNRS 7140, University of Strasbourg, Institut Le Bel, 4, rue Blaise Pascal, F-67000 Strasbourg, France.

^c A. E. Arbuzov Institute of Organic and Physical Chemistry, Russian Academy of Science, Arbuzov str. 8, Kazan 420088, Russian Federation

^d Université de Carthage, Laboratoire d'Application de la Chimie aux Ressources et Substances Naturelles et à l'Environnement (LACReSNE), unité des interactions moléculaires spécifiques, Faculté des Sciences de Bizerte, 7021 Bizerte, Tunisia

E-mail: ferlay@unistra.fr, hosseini@unistra.fr

- [1] a) G. D. Desiraju, *Crystal Engineering: The Design of Organic Solids*, Elsevier, New York, 1989; b) C.B. Aakeroy and K.R. Seddon, *Chem. Soc. Rev.*, 1993, **22**, 397; c) D. Braga, *Angew. Chem., Int. Ed.* 2004, **43**, 2; d) Ö. Almarsson; M. J. Zaworotko, *Chem. Commun.* 2004, 1889; e) G. R. Desiraju; J. J. Vittal; A. Ramanan *Crystal Engineering: A Text Book*; World Scientific: Singapore; f) A. D. Bond *CrystEngComm* 2012, **14**, 2363.
- [2] Lehn, J.-M. *Supramolecular Chemistry, Concepts and Perspectives*, VCH, Weinheim, 1995.
- [3] (a) J. D. Dunitz, *Pure and Appl. Chem.* 1991, **63**, 177; (b) J. D. Dunitz, *Chem. Commun.*, 2003, 545.
- [4] a) S. Mann, *Nature*, 1993, **365**, 499; b) M. Simard, D. Su, J. D. Wuest, *J. Am. Chem. Soc.*, 1991, **113**, 4696; c) M. W. Hosseini, *Acc. Chem. Res.* 2005, **38**, 313.
- [5] A. F. Wells, *Three-dimensional Nets and Polyhedra*, Wiley-Interscience, New York, 1977; Further Studies of Three-dimensional Nets, ACA Monograph No. 8, American Crystallographic Association, 1979.
- [6] M. W. Hosseini, *CrystEngComm.*, 2004, **6**, 318.
- [7] a) J. D. Wuest, *Chem. Commun.*, 2005, 5830; b) M. W. Hosseini, *Chem. Commun.*, 2005, 5825.
- [8] (a) B. F. Abrahams, B. F. Hoskins, R. Robson, *J. Am. Chem. Soc.*, 1991, **113**, 3606; (b) S. R. Batten, R. Robson, *Angew. Chem. Int. Ed.*, 1998, **37**, 1460.
- [9] a) C. Kaes, M. W. Hosseini, NATO ASI Series, Ed. J. Viciano, 1998, **C518**, 53; b) M. W. Hosseini, NATO ASI Series, Ed. G. Tsoucaris, 1998, **C519**, 209; c) M. W. Hosseini, NATO ASI Series, Eds. D. Braga, G. Orpen, Serie c, 1999, **C538**, 181.
- [10] (a) O. M. Yaghi, H. Li, C. Davis, D. Richardson, T. L. Groy, *Acc. Chem. Res.*, 1998, **31**, 474; (b) M. Eddaoudi, D. B. Moler, H. Li, B. Chen, T.M. Reineke, M. O'Keeffe, O. M. Yaghi, *Acc. Chem. Res.*, 2001, **34**, 319.
- [11] (a) A. J. Blake, N. R. Champness, P. Hubberstey, W.-S. Li, M. A. Withersby, M. Schröder, *Coord. Chem. Rev.*, 1999, **193**, 117; (b) B. Moulton, M. J. Zaworotko, *Chem. Rev.*, 2001, **101**, 1629; (c) C. Janiak, *Dalton Trans.*, 2003, 2781; (d) L. Carlucci, G. Ciani, D. M. Proserpio, *Coord. Chem. Rev.*, 2003, **246**, 247; (e) S. Kitagawa, R. Kitaura, S. Noro, *Angew. Chem. Int. Ed.*, 2004, **43**, 2334; (f) G. Férey, C. Mellot-Draznieks, C. Serre, F. Millange, *Acc. Chem. Res.*, 2005, **38**, 218; (g) D. Bradshaw, J. B. Claridge, E. J. Cussen, T. J. Prior, M. J. Rosseinsky, *Acc. Chem. Res.*, 2005, **38**, 273; (h) S. Kitagawa, K. Uemura, *Chem. Soc. Rev.* 2005, **34**, 109; (i) D. Maspocho, D. Ruiz-Molina, J. Veciana, *Chem. Soc. Rev.* 2007, **36**, 770; (j) J. R. Long, O. M. Yaghi, *Chem. Soc. Rev.*, 2009, **38**, 1213; (k) C. Janiak, J. L. Vieth, *New J. Chem.*, 2010, **34**, 2366; (l) *Chem. Soc. Rev.*, 2009, **38**, themed issue on metal-organic frameworks; (m) W. L. Leong, J. J. Vittal, *Chem. Rev.* 2011, **111**, 688; (n) *Chem. Rev.*, 2012, **112**, Metal-Organic Frameworks special issue.
- [12] (a) C.D. Gutsche in *Calixarenes Revised: Monographs in Supramolecular Chemistry Vol. 6*, The Royal Society of Chemistry, Cambridge, 1998; (b) Z. Asfari, V. Böhmer, J. Harrowfield, J. Vicens in *Calixarenes 2001*, (Eds. Z. Asfari, V. Böhmer, J. Harrowfield, J. Vicens) Kluwer Academic, Dordrecht, 2001.
- [13] (a) H. Kumagai, M. Hasegawa, S. Miyanari, Y. Sugawa, Y. Sato, T. Hori, S. Ueda, H. Kamiyama, S. Miyano, *Tetrahedron Lett.*, 1997, **38**, 3971; (b) H. Akdas, L. Bringel, E. Graf, M. W. Hosseini, G. Mislin, J. Pansanel, A. De Cian, J. Fischer, *Tetrahedron Lett.*, 1998, **39**, 2311.
- [14] (a) C. G. Gibbs, C. D. Gutsche, *J. Am. Chem. Soc.*, 1993, **115**, 5338; (b) C. G. Gibbs, P. K. Sujeeth, J. S. Rogers, G. G. Stanley, M. Krawiec, W. H. Watson, C. D. Gutsche, *J. Org. Chem.*, 1995, **60**, 8394.
- [15] X. Delaigue, J. McB. Harrowfield, M. W. Hosseini, A. De Cian, J. Fischer, N. Kyritsakas, *Chem. Commun.*, 1994, 1579.
- [16] P. Rao, M. W. Hosseini, A. De Cian, J. Fischer, *Chem. Commun.*, 1999, 2169.
- [17] M. W. Hosseini in *Calixarenes 2001*, (Eds. Z. Asfari, V. Böhmer, J. Harrowfield, J. Vicens) Kluwer Academic, Dordrecht, 2001, pp.110.
- [18] (a) G. Mislin, E. Graf, M. W. Hosseini, A. Bilyk, A. K. Hall, J. M. Harrowfield, B. W. Skelton, A. H. White, *Chem. Commun.*, 1999, 373; (b) H. Akdas, E. Graf, M. W. Hosseini, A. De Cian, A. Bilyk, B. W. Skelton, G. A. Koutsantonis, I. Murray, J. M. Harrowfield, A. H. White, *Chem. Commun.*, 2002, 1042; (c) A. Bilyk, J. W. Dunlop, R. O. Fuller, A. K. Hall, J. M. Harrowfield, M. W. Hosseini, G. A. Koutsantonis, I. W. Murray, B. W. Skelton, A. N. Sobolev, R. L. Stamps, A. H. White, *Eur. J. Inorg. Chem.* 2010, 2127; (d) A. Bilyk, J. W. Dunlop, R. O. Fuller, A. K. Hall, J. M. Harrowfield, M. W. Hosseini, G. A. Koutsantonis, I. W. Murray, B. W. Skelton, R. L.

- Stamps, A. H. White, *Eur. J. Inorg. Chem.* 2010, 2106; (e) A. Bilyk, J. W. Dunlop, R. O. Fuller, A. K. Hall, J. M. Harrowfield, M. W. Hosseini, G. A. Koutsantonis, I. W. Murray, B. W. Skelton, A. N. Sobolev, R. L. Stamps, A. H. White *Eur. J. Inorg. Chem.* 2010, 2106; (f) A. Gehin, S. Ferlay, J. M. Harrowfield, D. Fenske, N. Kyritsakas and M. W. Hosseini, *Inorg. Chem.*, 2012, **51**, 5481.
- [19] (a) T. Kajiwara, N. Kon, S. Yokozawa, T. Ito, N. Iki, S. Miyano, *J. Am. Chem. Soc.* 2002, **124**, 11274; (b) C. Desroches, G. Pilet, S. A. Borsch, S. Parola, D. Luneau, *Inorg. Chem.* 2005, **44**, 9112; (c) Y. F. Bi, X. T. Wang, W. P. Liao, X. W. Wang, R. P. Deng, H. J. Zhang, S. Gao, *Inorg. Chem.* 2009, **48**, 11743; (d) Y. Bi, X-T. Wang, W. Liao, X. Wang, X. Wang, H. Zhang, S. Gao, *J. Am. Chem. Soc.* 2009, **131**, 11650.
- [20] T. Kajiwara, N. Iki, M. Yamashita, *Coord. Chem. Rev.* 2007, **251**, 1734.
- [21] M. N. Kozlova, S. Ferlay, S. E. Solovieva, I. S. Antipin, A. I. Kononov, N. Kyritsakas, M. W. Hosseini, *Dalton Trans.*, 2007, 5126.
- [22] H. Akdas, E. Graf, M. W. Hosseini, A. De Cian, J. M. Harrowfield, *Chem. Commun.*, 2000, 2219.
- [23] M. N. K. Kozlova, S. Ferlay, N. Kyritsakas, M. W. Hosseini, S. E. Solovieva, I. S. Antipin, A. I. Kononov, *Chem. Commun.*, 2009, 2514.
- [24] J. Sykora, M. Himl, I. Stobor, I. Cisarova, P. Lhotak, *Tetrahedron*, 2007, **63**, 2244.
- [25] Y. Bi, W. Liao, X. Wang, R. Deng and H. Zhang, *Eur. J. Inorg. Chem.*, 2009, 4989.
- [26] (a) K. Kim, S. Park, K-M. Park and S. S. Lee, *Cryst. Growth Des.*, 2011, **11**, 4059; (b) M. Liu and W. Liao, *Chem. Commun.*, 2012, 5727.
- [27] (a) K. Hirata, T. Suzuki, A. Noya, I. Takei, M. Hidai, *Chem. Commun.* 2005, 3718 ; (b) D. Buccella, G. Parkin, *Chem. Commun.* 2009, 289.
- [28] a) A. Ovsyannikov, S. Ferlay, S. E. Solovieva, I. S. Antipin, A. I. Kononov, N. Kyritsakas, M. W. Hosseini, *Inorg. Chem.*, 2013, **52**, 6776 ; b) A. Ovsyannikov, S. Ferlay, S. E. Solovieva, I. S. Antipin, A. I. Kononov, N. Kyritsakas, M. W. Hosseini, *Dalton*, 2013, **42**, 9946.
- [29] a) A. Ovsyannikov, M. N. Lang, S. Ferlay, S. E. Solovieva, I. S. Antipin, A. I. Kononov, N. Kyritsakas, M. W. Hosseini, *Dalton Trans.*, 2013, **42**, 116; b) A. Ovsyannikov, S. Ferlay, S. E. Solovieva, I. S. Antipin, A. I. Kononov, N. Kyritsakas, M. W. Hosseini, *Dalton Trans.*, 2014, **43**, 158; c) A. Ovsyannikov, S. Ferlay, S. E. Solovieva, I. S. Antipin, A. I. Kononov, N. Kyritsakas, M. W. Hosseini, *CrystEngComm*, 2014, 3765.
- [30] A. Ovsyannikov, S. Ferlay, S. E. Solovieva, I. S. Antipin, A. I. Kononov, N. Kyritsakas, M. W. Hosseini, *Russian Chem. Bull.*, 2014, accepted, rus. *Известия Академии Наук, Серия химическая*, ISSN 0002-3353, 2015, **8**, 1955-1962.
- [31] N. Iki, C. Kabuto, T. Fukushima, H. Kumagai, H. Takeya, S. Miyanari, T. Miyashib and S. Miyano, *Tetrahedron*, 2000, **56**, 1437.
- [32] C. Blaszykowski, E. Aktoudianakis, C. Bressy, D. Alberico and M. Lautens, *Org. Lett.*, 2006, **8**, 2043.
- [33] I. Bitter, V. Csokai, *Tetrahedron Lett.*, 2003, **44**, 2261.
- [34] H. Akdas, L. Bringel, V. Bulach, E. Graf, M. W. Hosseini, A. De Cian, *Tetrahedron Letters*, 2002, **43**, 8975.
- [35] G. M. Sheldrick, Program for Crystal Structure Solution, University of Göttingen, Göttingen, Germany, 1997. □
- [36] a) K. Paek, J. Yoon and Y. Suh, *J. Chem. Soc., Perkin Trans. 2*, 2001, 916; b) R. Zadnarm, M. Junkers, T. Schrader, T. Grawe and A. Kraft, *J. Org. Chem.* 2003, **68**, 6511.
- [37] a) J. Ehrhart, J-M. Planeix, N. Kyritsakas-Gruber, M. W. Hosseini, *Dalton Trans.*, **2009**, 6309; b) J. Ehrhart, J-M. Planeix, N. Kyritsakas-Gruber, M. W. Hosseini, *Dalton Trans.*, 2009, 2557; c) J. Ehrhart, J-M. Planeix, N. Kyritsakas-Gruber, M. W. Hosseini, *Dalton Trans.*, 2010, 2137.
- [38] a) C. Klein, E. Graf, M. W. Hosseini, A. De Cian and J. Fischer, *Chem. Commun.*, 2000, 239; b) G. Laugel, E. Graf, M. W. Hosseini, J.-M. Planeix and N. Kyritsakas, *New J. Chem.*, 2006, **30**, 1340.

ARTICLE

Table 1: Crystallographic data for structural analyses of **3** and **6**

Formula	3	6
	$C_{60}H_{72}N_8O_4S_4, H_2O$	$C_{60}H_{72}N_8S_8$
Molecular weight	1115.51	1161.73
Crystal system	monoclinic	monoclinic
Space group	P2(1)/c	C12/c1
a(Å)	15.2164(12)	26.6378(6)
b(Å)	13.1809(10)	12.7707(3)
c(Å)	29.309(2)	19.6019(4)
α (deg)	90	90
β (deg)	92.577(3)	115.0020(10)
γ (deg)	90	90
V(Å ³)	5872.5(8)	6043.4(2)
Z	4	4
Colour	Colourless	Colourless
Crystal dim (mm ³)	0.06 x 0.06 x 0.05	0.040 x 0.050 x 0.050
Dcalc (gcm ⁻³)	1.262	1.277
F(000)	2376	2464
μ (mm ⁻¹)	0.217	0.341
Wavelength (Å)	0.71073	0.71073
Number of data meas.	41169	20696
Number of data with $I > 2\sigma(I)$	16909 [R(int) = 0.0427]	7884 [R(int) = 0.0235]
R	R1 = 0.1114, wR2 = 0.2497	R1 = 0.0479, wR2 = 0.1393
Rw	R1 = 0.1732, wR2 = 0.2668	R1 = 0.0680, wR2 = 0.1568
GOF	1.124	1.004
Largest peak in final difference (eÅ ⁻³)	1.069 and -0.689	0.732 and -0.720

$${}^a R = \Sigma(|F_o| - |F_c|) / \Sigma |F_o|; {}^b wR = [\Sigma[w(F_o^2 - F_c^2)^2] / \Sigma w(F_o^2)^2]^{1/2}$$

COMMUNICATION

Table 3: Crystallographic data for structural analyses for 5-AgSbF₆, 5-AgBF₄, 6-AgBF₄, 6-AgPF₆, 6-AgSbF₆, 6-AgAsF₆, 7-AgSbF₆, 8-AgNO₃, 8-AgSbF₆

Formula	5-AgSbF ₆ C ₆₈ H ₈₈ N ₈ O ₄ S ₄ , AgSbF ₆ , CHCl ₃	5-AgBF ₄ C ₆₈ H ₈₈ N ₈ O ₄ S ₄ , AgBF ₄ , 3H ₂ O	6-AgBF ₄ 2(C ₃₀ H ₃₆ N ₄ S ₄), 2(AgBF ₄), H ₂ O	6-AgPF ₆ C ₃₀ H ₃₆ N ₄ S ₄ AgPF ₆ , 3H ₂ O	6-AgSbF ₆ C ₃₀ H ₃₆ N ₄ S ₄ AgSbF ₆ , 3H ₂ O	6-AgAsF ₆ C ₃₀ H ₃₆ N ₄ S ₄ AgAsF ₆ , 3H ₂ O	7-AgSbF ₆ C ₆₄ H ₈₀ N ₈ S ₈ , (AgSbF ₆) ₂ , 2 CHCl ₃	8-AgNO ₃ C ₃₄ H ₄₆ N ₄ S ₄ AgNO ₃ H ₂ O	8-AgSbF ₆ 2(C ₆₈ H ₈₈ N ₈ S ₈), 4(AgSbF ₆), 7(CHCl ₃), 2(H ₂ O)
Molecular weight	1672.69	1458.43	1569.11	887.75	978.53	931.70	2143.82	824.87	4793.96
Crystal system	monoclinic	monoclinic	tetragonal	tetragonal	tetragonal	tetragonal	triclinic	monoclinic	triclinic
Space group	P2(1)/c	Cc	I 41/a	I 41/a	I 41/a	I 41/a	P-1	C 2/c	P-1
a(Å)	16.8948(3)	22.7969(11)	16.0983(5)	24.2538(9)	24.958(3)	24.4165(8)	15.6888(4)	36.0428(10)	18.8461(13)
b(Å)	14.6737(3)	17.2741(8)	16.0983(5)	24.2538(9)	24.958(3)	24.4165(8)	17.4322(5)	12.4438(3)	19.0515(11)
c(Å)	30.1055(6)	19.4952(9)	54.7728(15)	13.6809(5)	13.8496(19)	13.7457(4)	17.6605(5)	20.2117(7)	19.1473(10)
α(deg)	90	90	90	90	90	90	80.5980(10)	90	99.994(3)
β(deg)	90.7060(10)	103.7860(9)	90	90	90	90	76.5880(10)	121.0560(17)	113.120(2)
γ(deg)	90	90	90	90	90	90	71.0250(10)	90	115.1260(17)
V(Å ³)	7462.9(3)	7456.0(6)	14194.7(10)	8047.7(7)	8627.(2)	8194.7(6)	4422.6(2)	7765.8(4)	5224.5(6)
Z	4	4	8	8	8	8	2	8	1
Colour	Colourless	Colourless	Colourless	Colourless	Colourless	Colourless	Colourless	Colourless	Colourless
Crystal dim (mm ³)	0.07 x 0.06 x 0.06		0.050 x 0.050 x 0.060	0.060 x 0.060 x 0.070	0.060 x 0.060 x 0.070	0.050 x 0.050 x 0.060	0.08 x 0.06 x 0.06	0.050 x 0.060 x 0.060	0.050 x 0.050 x 0.060
Dcalc (gcm ⁻³)	1.489	1.299	1.468	1.465	1.507	1.510	1.610	1.411	1.524
F(000)	3432	3064	6416	3632	3920	3776	2136	3424	2394
μ (mm ⁻¹)	0.910	0.447	0.853	0.811	1.332	1.558	1.477	0.776	1.371
Wavelength (Å)	0.71073	0.71073	0.71073	0.71073	0.71073	0.71073	0.71073	0.71073	0.71073
Number of data meas.	247880	32679	116099	104738	22682	97274	176449	32086	57782
Number of data with I > 2σ(I)	23255 [R(int) = 0.0454]	20781 [R(int) = 0.0340]	10377 [R(int) = 0.0894]	5185 [R(int) = 0.0318]	6216 [R(int) = 0.0557]	6060 [R(int) = 0.0304]	23624 [R(int) = 0.0365]	11147 [R(int) = 0.0381]	25186 [R(int) = 0.0321]
R	R1 = 0.0591, wR2 = 0.1543	R1 = 0.0829, wR2 = 0.2117	R1 = 0.0796, wR2 = 0.2152	R1 = 0.0495, wR2 = 0.1563	R1 = 0.1092, wR2 = 0.3064	R1 = 0.0485, wR2 = 0.1444	R1 = 0.0646, wR2 = 0.1905	R1 = 0.0573, wR2 = 0.1489	R1 = 0.0713, wR2 = 0.2203
Rw	R1 = 0.0806, wR2 = 0.1704	R1 = 0.1232, wR2 = 0.2471	R1 = 0.1221, wR2 = 0.2376	R1 = 0.0535, wR2 = 0.1644	R1 = 0.1457, wR2 = 0.3320	R1 = 0.0602, wR2 = 0.1516	R1 = 0.0973, wR2 = 0.2215	R1 = 0.0819, wR2 = 0.1650	R1 = 0.0990, wR2 = 0.2441
GOF	1.023	1.022	1.078	1.009	1.005	1.008	1.034	1.048	1.080
Largest peak in final difference (eÅ ⁻³)	4.498 and -2.745	2.163 and -0.799	2.347 and -2.478	1.445 and -0.457	1.985 and -1.355	1.316 and -0.838	1.941 and -1.804	1.264 and -1.360	1.937 and -1.603